EPJ Web of Conferences **164**, 07006 (2017) DOI: 10.1051/epjconf/201716407006
ICNFP 2016

Beauty production measurements in pp, p–Pb and Pb–Pb collisions with the ALICE detector

Minjung Kim for the ALICE collaboration[1,a]

[1] *Inha University, Incheon, Republic of Korea*

Abstract. Beauty production has been measured in the ALICE experiment via its semi-electronic decays and non-prompt J/ψ at mid-rapidity. A review of results on beauty production at mid-rapidity in pp collisions at $\sqrt{s}$ = 7 TeV and at $\sqrt{s}$ = 2.76 TeV, in p-Pb collisions at $\sqrt{s_{\rm NN}}$ = 5.02 TeV and in Pb-Pb collisions at $\sqrt{s_{\rm NN}}$ = 2.76 TeV are reported, along with the current status of b-jet tagging studies in ALICE. Prospects of beauty production measurements with RUN2 and RUN3-4 are outlined, focusing on the upgraded Inner Tracking System (ITS) and the new Muon Forward Tracker (MFT).

1 Introduction

In ultra-relativistic heavy-ion collisions, the hot and dense medium of colour-deconfined quarks and gluons, called Quark-Gluon plasma (QGP), is expected to be created with a formation of $\tau_{\rm QGP} \sim 0.3\,{\rm fm}/c$ and a of lifetime $\sim 10\,{\rm fm}/c$ at LHC energies [1, 2]. Heavy quarks (charm and beauty) are predominantly produced in the early stages of the collisions via initial hard scattering processes due to their large masses ($m_{\rm Q} \gg \Lambda_{\rm QCD}$) [3]. Since the time-scale of their formation is expected to be smaller than $\tau_{\rm QGP}$, heavy quarks can propagate through the QGP medium and experience the full system evolution, interacting with its constituents and loosing part of their energy within the medium. According to Quantum Chromodynamics (QCD), due to their smaller colour coupling to the medium with respect to gluons, the medium-induced parton energy loss of quarks is smaller than that of gluons [4–6]. Additionally, theoretical model calculations predict the mass dependence of medium-induced parton energy loss in radiative energy loss process [7–9] and collisional energy loss process [10]. In many models, the mass-dependence of parton energy loss is given as a function of m/E and it becomes negligible when the ratio m/E approaches to zero. Consequently, beauty quarks can be sensitive probes for testing the mass dependence of medium-induced parton energy loss in broader parton energy range with respect to charm quarks [11].

The sensitive observable for investigating the medium-induced parton energy loss is the nuclear modification factor ($R_{\rm AA}$), which is defined as the ratio of the yield in Pb-Pb collisions to that observed in the pp collisions scaled by the average number of binary collisions. $R_{\rm AA}$ of heavy-flavour hadrons in comparison with $R_{\rm AA}$ of light-flavour hadrons indicate possible colour-charge and mass dependence of medium-induced energy loss. For that reason, the measurements of open heavy-flavour hadron yields in pp collisions are essential, as the references for corresponding measurements in Pb-Pb collisions. In addition, the measurements in pp collisions provide the tests of perturbative Quantum

[a] e-mail: minjung.kim@cern.ch

Chromodynamics (pQCD) calculations. The $R_{\rm AA}$ measurements possess not only the final-state effects from hot and dense medium, but also the initial-state effects due to the presence of nuclei, so called cold nuclear matter (CNM) effect. Similar to $R_{\rm AA}$ in Pb-Pb collisions, the nuclear modification factor $R_{\rm pA}$, defined as the ratio of the yield in p-Pb collisions to that observed in the pp collisions scaled by the number of nucleons in the nucleus, can quantify the possible CNM effects, such as the modification of parton distribution functions in the nucleus [12] and the transverse momentum broadening from multiple scattering [13].
ALICE (A Large Ion Collider Experiment) at the LHC is dedicated to studying the QGP properties [14]. The central barrel detectors of ALICE provide electron identification capability down to very low $p_{\rm T}$ and excellent momemtum and track impact parameter resolution [15, 16]. Accordingly, beauty-hadron production at mid-rapidity have been measured via electrons from semi-leptonic decays of beauty hadrons and J/ψ from weak decays of beauty hadrons (non-prompt J/ψ) through di-electron decay channel, exploiting displaced secondary vertices of beauty hadrons due to their long lifetime ($c\tau \sim 500\,\mu$m). As a complementary approach in different kinematic range, the measurements of jets coming from beauty-quark fragmentation (b-jet) are ongoing.
In the following, the review of results on beauty production at mid-rapidity in pp collisions at $\sqrt{s} = 7$ TeV and $\sqrt{s} = 2.76$ TeV, in p-Pb collisions at $\sqrt{s_{\rm NN}} = 5.02$ TeV and in Pb-Pb collisions at $\sqrt{s_{\rm NN}} = 2.76$ TeV from data collected during the LHC-RUN1 are presented, together with the status of b-jet analysis. Prospects of beauty production measurements with RUN2 and RUN3-4 are outlined, focusing on the upgraded Inner Tracking System (ITS) and the new Muon Forward Tracker (MFT), which will be installed during the second long shutdown (LS2) between RUN2 and RUN3 [17].

2 Measurements of beauty production in ALICE

For charged particles reconstruction, the Inner Tracking System (ITS), which consists of 6-layered silicon detector and Time Projection Chamber (TPC) are used, together with a magnetic field of 0.5 T [14]. They provide a transverse momentum ($p_{\rm T}$) resolution better than 2.5% for $p_{\rm T} \leq 30$ GeV/c and transverse impact parameter (d_0) resolution better than 75 μm for $p_{\rm T} > 1$ GeV/c, where the d_0 is defined as the track distance of closest approach to the primary vertex in the plane transverse to the beam axis [18]. For measurements of electrons from beauty-hadron decays and of non-prompt J/ψ, electrons were identified using specific energy loss (dE/dx) measured in the TPC. The ITS, Time-Of-Flight (TOF) detector or Electromagnetic Calorimeter (EMCal) were additionally used for measurements of electrons from beauty-hadron decays, depending on the collision systems and the $p_{\rm T}$ ranges. V0 scintillator arrays located at $-3.7 < \eta < -1.7$ and at $2.8 < \eta < 5.1$ were used for centrality determination in Pb-Pb measurements.

2.1 Electrons from beauty-hadron decays

The long lifetime of beauty hadrons leads to larger d_0 of electrons from beauty-hadron decays than those of background electrons, which are mainly from Dalitz decays of light-neutral mesons, from conversions of photons in the detector materials and from semi-electronic decays of charm hadrons. After electron identification two different analysis methods, exploiting the distinguishable d_0 distributions of electrons from different origins, were applied to extract electrons from beauty-hadron decays. In pp collisions and p-Pb collisions, the signal were extracted by requiring minimum d_0 for electron candidates to increase signal to backgroud ratio and subtracting remaining background electrons, which were estimated based on ALICE measured hadron spectra [19–21]. In Pb-Pb collisions, the signal was extracted by fitting d_0 distribution of electron candidates with signal and background

templates, obtained from the Monte Carlo simulations. The correction on d_0 distributions in Monte Carlo simulations was done based on data. For instance, p_{T} spectra of charm hadrons in Monte Carlo simulations were re-weighted using the ALICE measured D meson spectrum [22]. The remaining uncertainty from imperfection of Monte Carlo simulations on describing data was propagated to the systematic uncertainties [21].

Apart from the methods based on impact parameter, the relative contribution of beauty to the electrons from heavy-flavour decays could be measured using azimuthal angular correlation of electrons from heavy-flavour decays to charged hadrons. The width of the near-side peak in the correlation distribution is broader for beauty-hadron decays than for charm-hadron decays due to the their different decay kinematics. The fraction of electrons from beauty-hadron decays in inclusive heavy-flavour decays electrons was extracted by fitting the correlation distribution with Monte Carlo templates [20].

In pp collisions, the p_{T}-differential invariant cross section of electrons from beauty-hadron decays in $|y| < 0.8$ was measured at $\sqrt{s} = 7$ TeV and at $\sqrt{s} = 2.76$ TeV as shown in Figure 1 are well described by pQCD-based calculations within the experimental and theoretical uncertainties.

In p-Pb collisions and in the 20% most central Pb-Pb collisions, the nuclear modification factor (R_{pPb} and R_{AA}, respectively) was measured as a function of p_{T} as shown in Figure 2. Within uncertainties,

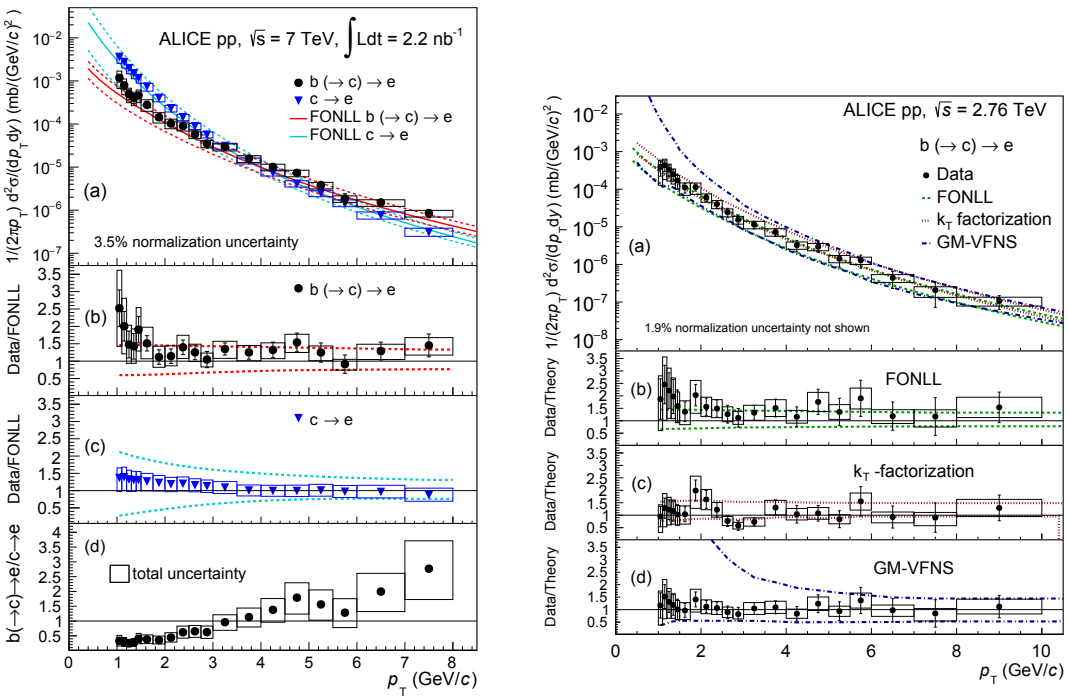

Figure 1: Production cross section of electrons from beauty- and charm-hadron decays and their ratio in pp collisions at $\sqrt{s} = 7$ TeV [19], compared to Fixed-Order plus Next-to-Leading Log (FONLL) pQCD calculations [23] (left), and production cross section of electrons from beauty-hadron decays in pp collisions at $\sqrt{s} = 2.76$ TeV [20], compared to FONLL [23], k_{T}-factorization [24] and GM-VFNS [25] predictions (right).

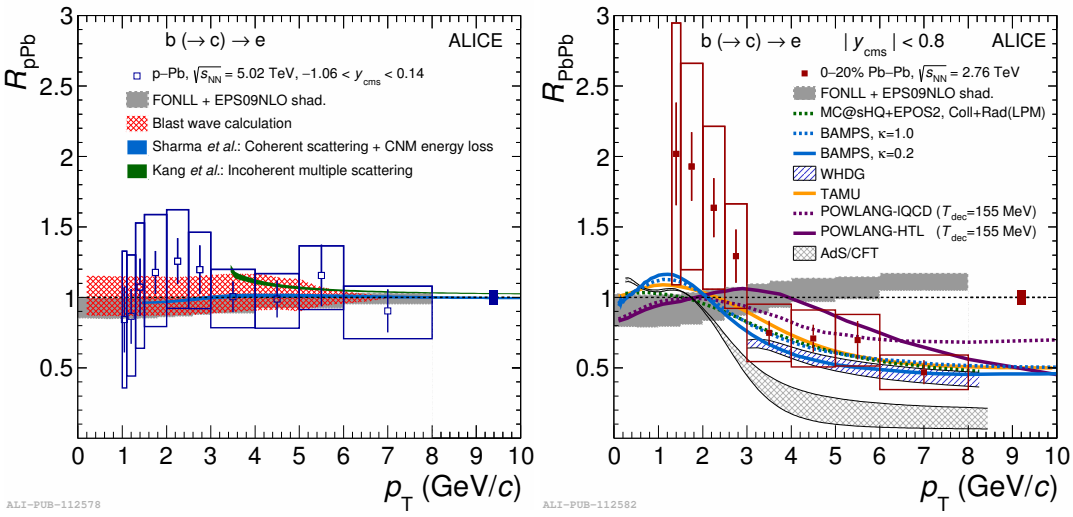

Figure 2: Nuclear modification factor of electrons from beauty-hadron decays at mid-rapidity in p-Pb collisions at $\sqrt{s_{\rm NN}} = 5.02\,\text{TeV}$ (left) and in Pb-Pb collisions at $\sqrt{s_{\rm NN}} = 2.76\,\text{TeV}$ in the 20% most central collisions (right) with different theoretical predictions [21]. The normalization uncertainty is shown as a filled box for both plots.

the $R_{\rm pPb}$ is compatible with unity and is well described by theoretical predictions, such as FONLL pQCD calculations [23, 26, 27] with the EPS09NLO nPDF parameterisation [12], model calculations including CNM energy loss, nuclear shadowing and mutiple scattering [28, 29] and blast-wave model calculations considering possible hydrodynamic effects [30]. The $R_{\rm AA}$ shows the suppression of electrons from beauty-hadron decays in the 20% most central Pb-Pb collisions with respect to pp collisions for $p_{\rm T} > 3\,\text{GeV}/c$. Therefore, the suppression of electrons from beauty-hadron decays for $p_{\rm T} > 3\,\text{GeV}/c$ in the 20% most central Pb-Pb collisions can be interpreted as an effect of the hot and dense medium on beauty quarks.

2.2 Non-prompt J/ψ

The long lifetime of beauty hadrons leads to larger flight distance of J/ψ from the decay of beauty hadrons than prompt J/ψ, which are direct produced in collisions and J/ψ from decays of heavier charmonium states. Consequently, non-prompt J/ψ is more likely to have large and positive pseudo-proper decay length (x), which is defined as $x = \frac{c \cdot L_{xy} \cdot m_{J/\psi}}{p_{\rm T}^{J/\psi}}$, where $L_{\rm xy}$ is the projection of the flight distance onto its transverse momentum vector and $m_{J/\psi}$ is the mass of the J/ψ. After electron identification, an unbinned 2-dimensional simultaneous fit for invariant mass distributions of J/ψ and x was used to determine the ratio of non-prompt to inclusive J/ψ [31].
The fraction of non-prompt J/ψ measured in pp collisions at $\sqrt{s} = 7\,\text{TeV}$ and in Pb-Pb collisions at $\sqrt{s_{\rm NN}} = 2.76\,\text{TeV}$ is presented in left panel of Figure 3 [31, 32]. The fraction in Pb-Pb collisions has a similar $p_{\rm T}$ dependence as in pp collisions. It is an open question whether the similarity comes from compensation of the medium effects on the prompt J/ψ, such as J/ψ dissociation and recombination or from medium-induced effects on the non-prompt J/ψ, related to beauty-quark energy loss, or from an interplay between those effects. Based on the measurement of inclusive J/ψ $R_{\rm AA}$ and the fraction of

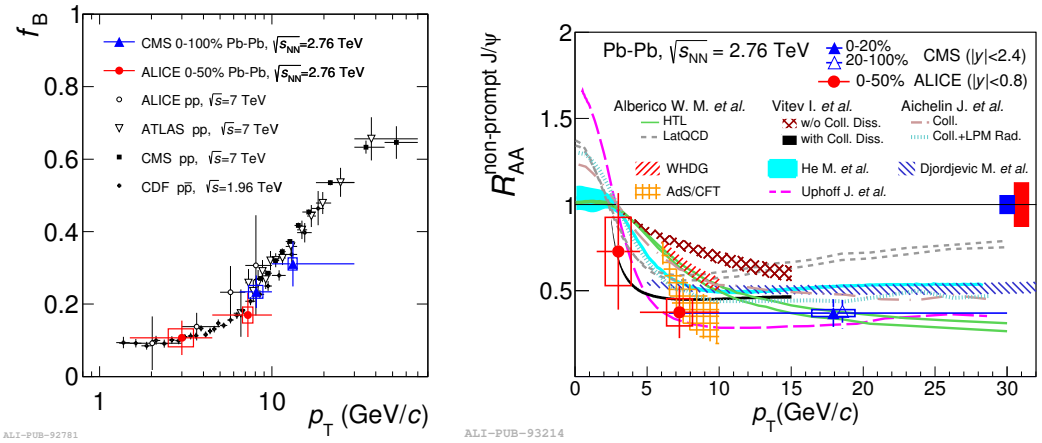

Figure 3: The fraction of J/ψ from the decay of beauty-hadrons measured at mid-rapidity in pp collisions and Pb-Pb collisions as a function of p_T compared with measurements by CMS [33, 34], ATLAS [35] and CDF [36] results (left) and the nuclear modification factor of J/ψ from the decay of beauty-hadrons at mid-rapidity in the 50% most central Pb-Pb collisions at $\sqrt{s_{NN}} = 2.76$ TeV together with CMS results [33] and theoretical predictions (right) [32].

non-prompt J/ψ, the R_{AA} of non-prompt J/ψ was obtained as shown in the right panel of Figure 3 [32]. The R_{AA} extends the kinematic coverage of CMS [33] down to low p_T. In $4.5 < p_T < 10\,\text{GeV}/c$, the suppression of non-prompt J/ψ tends to be stronger than what is predicted by most of the models.

2.3 b-jet

Tagging the jets coming from the fragmentation of beauty quarks (b-jet) represents an unbiased selection on the kinematics of the hard scattering, even in heavy-ion collisions. In addition, b-jet tagging with different jet radii allow the study of beauty-quark energy loss redistribution in Pb-Pb collisions. After jet reconstruction with charged tracks, b-jet can be identified exploiting long lifetime and large mass of beauty hadrons. In the following, two methods for b-jet tagging used in ALICE are presented. One way to tag b-jets among reconstucted jets is based on the signed impact parameter of the tracks in the reconstructed jet, where the sign of impact parameter is determined with the sign of the scalar product of the jet direction and the vector from primary vertex to the point of DCA. The tagging procedure considered using the signed impact parameter is the following. First, sort tracks in a jet by decreasing values of the signed impact parameter. Based on the fact that the probability to have several tracks with high positive signed impact parameter is high for b-jet due to the displaced secondary vertex of beauty hadron, assign the impact parameter of the N^{th} most displaced track as discriminator for a given jet and select jets which have large discriminator exceeding certain threshold (d_0). Here, N and d_0 are selected depending on the datasets since they should be optimised for S/B and statistical significance. In the left panel of Figure 4, the signed impact parameter distribution of the 3$^{\text{rd}}$ most displaced track in b-jet features distinct shape from that of c-jet.
The other way to tag b-jet is relied on the reconstruction of secondary vertex. After reconstructing secondary vertices (SV) with 2 or 3 tracks within a jet, use the signed flight distance significance ($L_{xy}/\sigma_{L_{xy}}$) and SV dispersion (σ_{vtx}) as discriminator of a given jet. As shown in middle panel of

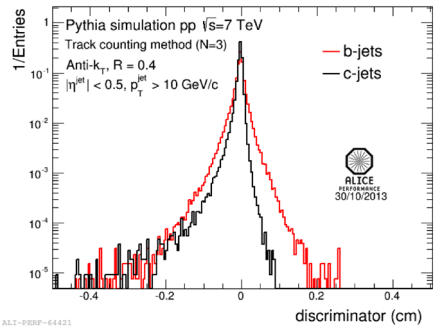

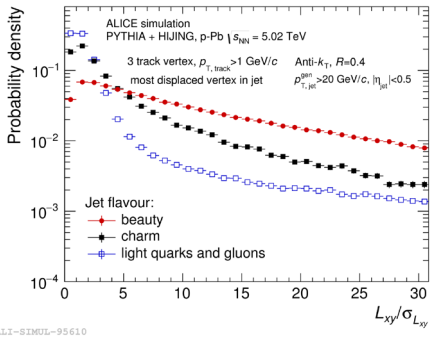

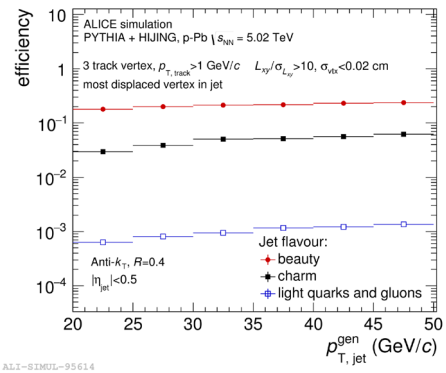

Figure 4: Signed impact parameter distributions of the 3rd most displaced track in given flavour jets in pp collisions at $\sqrt{s} = 7\,\text{TeV}$ (left, top), flight distance significance distributions of the most displaced secondary vertex found in given flavour jets in p-Pb collisions at $\sqrt{s_{\text{NN}}} = 5.02\,\text{TeV}$ (right, top) and b-jet tagging efficiency and mis-tagging rates based on reconstruction of secondary vertex in p-Pb collisions at $\sqrt{s_{\text{NN}}} = 5.02\,\text{TeV}$ (left, bottom). All plots are obtained from the Monte Carlo simulations.

Figure 4, $L_{\text{xy}}/\sigma_{L_{\text{xy}}}$ distribution of the most displaced SV in b-jet is broader compared to those in c-jet and jet from light quarks and gluons. σ_{vtx}, the dispersion of the tracks in the vertex, qualify the reconstructed secondary vertex. The right panel in Figure 4 shows the b-jet tagging efficiency and mis-tagging rates of c-jet and jet from light quarks and gluons calculated for requiring $L_{\text{xy}}/\sigma_{L_{\text{xy}}} > 10$ and $\sigma_{\text{vtx}} < 0.02\,\text{cm}$. They do not strongly vary with p_{T} and the b-tagging efficiency is higher about factor 100 compared to the jet from light quarks and gluons and about 3 to 5 compared to c-jet.

3 Prospects with RUN2 & RUN3

RUN2 of the LHC, from 2015 to 2018, offers the new higher collision energy for pp collisions up to $\sqrt{s} = 13\,\text{TeV}$ and for Pb-Pb collisions up to $\sqrt{s_{\text{NN}}} = 5\,\text{TeV}$. The increase of statistics compared to RUN1 allows to reduce not only statistical uncertainty but also systematic uncertainties. More precise beauty production measurements in an extended p_{T} coverage are expected.
Upgrading major detectors and computing framework is planned in LS2 between RUN2 and RUN3 [17]. Increase the readout capabilities of the detectors, especially TPC readout upgrade together with introducing new combined Online-Offline system for calibration and data compression, will increase the readout capabilities up to a rate of 50 kHz for Pb-Pb collisions and 200 kHz for pp and p-Pb collisions [37]. Improvement of tracking precision is expected via upgraded ITS at mid-rapidity and newly installed Muon Forward Tracker (MFT) at forward rapidity. As a result, better precision with more statistics and extended kinematic coverage measurements of beauty production

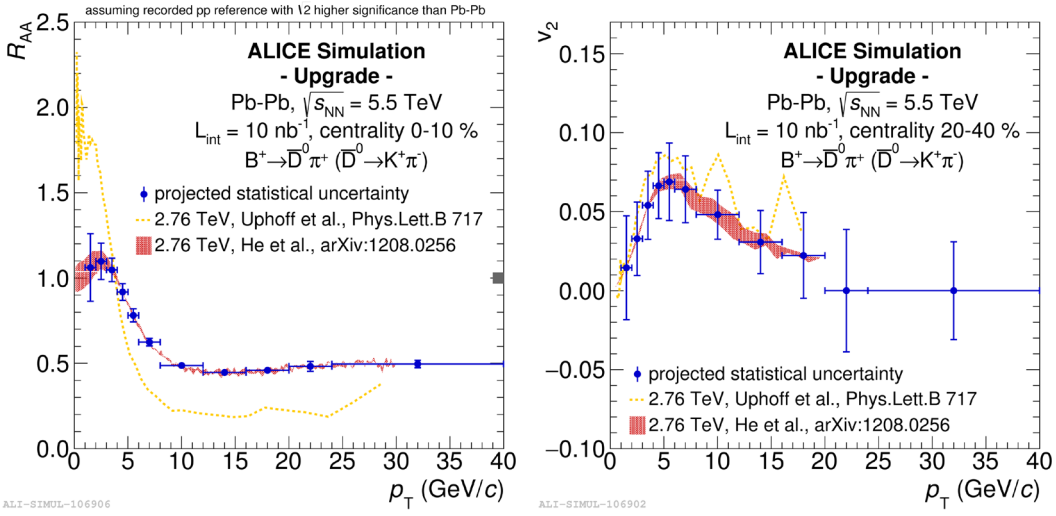

Figure 5: Nuclear modification factor of B^+ as a function of p_T compared to theoretical predictions (left) and azimuthal anisotropy, v_2 of B^+ as a function of p_T compared to theoretical predictions.(right)

with new observables will be possible. Brief description of upgraded ITS and MFT and their expected performances for beauty measurements are presented below.

3.1 Upgraded ITS

The upgraded ITS consists of 7 cylindrical layers of Monolithic Active Pixel Sensors (MAPS) [38]. The impact parameter resolution will be improved by a factor of 3 in $r\phi$-direction and 6 in z-direction with closer position of the first layer to interaction point (from r = 39 mm to r = 23 mm), reduced material budget (from $x/X_0 = 1.14$ % to $x/X_0 = 0.3$ %) and smaller pixel size (from 50 $\mu m \times 425$ μm to 28 $\mu m \times 28$ μm). The tracking efficiency and p_T resolution will be further improved by increasing layers from 6 to 7. Together with increased statistics in RUN3, more precise measurement of current observables such as R_{AA} of non-prompt J/ψ with extended p_T will be possible. Moreover, distinct decay topologies and kinematics allow for efficient full reconstruction of beauty-hadrons, for example, $B^+ \to D^0 + \pi^-$ ($D^0 \to K^+ + \pi^-$), $B^+ \to J/\psi + K^+$ ($J/\psi \to e^+ + e^-$) and $\Lambda_b^0 \to \Lambda_c^+ \pi^-$ ($\Lambda_c^+ \to pK^-\pi^+$). Figure 5 shows the expected R_{AA} and azimuthal anisotropy (v_2) of B^+ under the assumption of an integrated luminosity of $L_{int} = 10$ nb^{-1}.

3.2 MFT

In current ALICE apparatus, the muon spectrometer is blind to the details of the vertex region due to the hadron absorber. Muon Forward Tracker (MFT) composed with 5 layers (each layer consists of two half-disks) of silicon pixel sensors using same technology as the upgraded ITS will be installed during LS2 [39]. Muon tracks reconstructed in the muon spectrometer will be matching with the track segments reconstructed in MFT planes. High pointing accuracy of muons at forward rapidity region, which would be enough to separate muons from semi-leptonic decays of beauty-hadrons exploiting their displaced secondary vertex is expected. It also allows to measure non-prompt J/ψ down to $p_T = 0$ at forward rapidity as shown in Figure 6.

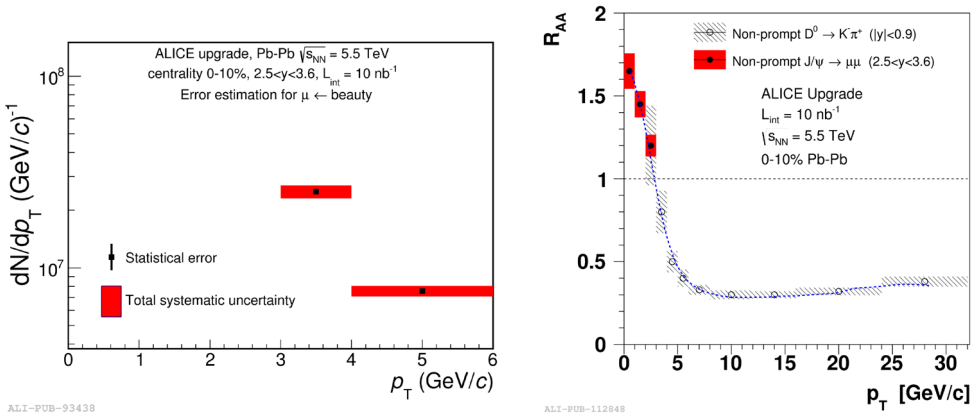

Figure 6: Transverse momentum distributions of muons from beauty-hadron decays (left) and nuclear modification factor of non-prompt J/ψ at forward rapidity compared with nuclear modification factor of non-prompt D^0 at mid-rapidity region (right) [39].

4 Conclusions

Thanks to the excellent tracking, vertexing and particle-identification capabilities provided by ALICE, beauty production is studied via semi-eletronic decay channels in pp, p-Pb and Pb-Pb collisions and non-prompt J/ψ in the e^+e^- decay channel in pp and Pb-Pb collisions at mid-rapidity.

The p_{T}-differential cross sections of electrons from beauty-hadron decays measured in pp collisions at $\sqrt{s} = 7$ TeV and $\sqrt{s} = 2.76$TeV are reproduced by several pQCD-based calculations. Since the R_{pA} of electrons from beauty-hadron decays is close to unity for $1 < p_{\mathrm{T}} < 8\,\mathrm{GeV}/c$, the suppression of R_{AA} shown in $p_{\mathrm{T}} > 3$ GeV/c provides a hint of the energy loss of beauty quarks in the hot and dense medium.

In the fraction of non-prompt J/ψ measured in Pb-Pb collisions, a similar p_{T} dependence as in pp collisions is observed. The suppression shown in R_{AA} of non-prompt J/ψ at $4.5 < p_{\mathrm{T}} < 10$ GeV/c tends to be stronger than what predicted by most of the models.

In order to study of in-medium energy loss of beauty without bias on the kinematics of the hard scattering and explore the energy loss redistribution of beauty quarks, b-jet tagging is ongoing in ALICE.

Better precision, more statistics and extended kinematic coverage measurements will be possible with the upcoming Run2 and RUN3-4 data. Especially after installation of the upgraded ITS and the MFT, beauty production measurements will be significantly improved with new observables, such as R_{AA} and v_2 of exclusively reconstructed beauty hadrons.

Acknowledgements

This work was supported by National Research Foundation of Korea (NRF), Basic Science Research Program through the National Research Foundation of Korea funded by the Ministry of Education, Science and Technology (Grant number: 2013S1A2A2035612) and by Inha University Research Grant (INHA-47297).

References

[1] F.M. Liu, S.X. Liu, Phys. Rev. C **89**, 034906 (2014)
[2] K. Aamodt et al., (ALICE Collaboration), Phys. Lett. **B696**, 328 (2013), arXiv:1012.4035
[3] A. Andronic et al., Eur. Phys. J. **C76**, 107 (2016), arXiv:1506.03981
[4] M. Gyulassy, X.N. Wang, Nucl. Phys. **B420**, 583 (1994), nucl-th/9306003
[5] R. Baier, Y.L. Dokshitzer, A.H. Mueller, S. Peigne, D. Schiff, Nucl. Phys. **B484**, 265 (1997), hep-ph/9608322
[6] U.A. Wiedemann, Nucl. Phys. **B588**, 303 (2000), hep-ph/0005129
[7] Y.L. Dokshitzer, D.E. Kharzeev, Phys. Lett. **B519**, 199 (2001), hep-ph/0106202
[8] M. Djordjevic, M. Gyulassy, Nucl. Phys. **A733**, 265 (2004), nucl-th/0310076
[9] N. Armesto, C.A. Salgado, U.A. Wiedemann, Phys. Rev. **D69**, 114003 (2004), hep-ph/0312106
[10] H. van Hees, V. Greco, R. Rapp, Phys. Rev. **C73**, 034913 (2006), 0508055
[11] N. Armesto, A. Dainese, C.A. Salgado, U.A. Wiedemann, Phys. Rev. D **71**, 054027 (2005)
[12] K.J. Eskola, H. Paukkunen, C.A. Salgado, JHEP **04**, 065 (2009), arXiv:0902.4154
[13] I. Vitev, Phys. Rev. C **75**, 064906 (2007)
[14] K. Aamodt et al., (ALICE Collaboration), JINST **3**, S08002 (2008)
[15] F. Carminati et al., (ALICE Collaboration), J. Phys. G: Nucl. Part. Phys. **30**, 1517 (2004)
[16] B. Alessandro et al., (ALICE Collaboration), J. Phys. G: Nucl. Part. Phys. **32**, 1295 (2004)
[17] B. Abelev et al., (ALICE Collaboration), J. Phys. G: Nucl. Part. Phys. **41**, 087001 (2014)
[18] B. Abelev et al., (ALICE Collaboration), Int. J. Mod. Phys. **A29**, 1430044 (2014), arXiv:1402.4476
[19] B. Abelev et al., (ALICE Collaboration), Phys. Lett. **B721**, 13 (2013), arXiv:1208.1902
[20] B. Abelev et al., (ALICE Collaboration), Phys. Lett. **B738**, 97 (2014), arXiv:1405.4144
[21] J. Adam et al., (ALICE Collaboration) (2016), arXiv:1609.03898
[22] B. Abelev et al., (ALICE Collaboration), JHEP **09**, 112 (2012), arXiv:1203.2160
[23] M. Cacciari, S. Frixione, N. Houdeau, M.L. Mangano, P. Nason, G. Ridolfi, Journal of High Energy Physics **2012**, 1 (2012)
[24] R. Maciuła, A. Szczurek, Phys. Rev. D **87**, 094022 (2013)
[25] P. Bolzoni, G. Kramer, Nucl. Phys. B **872**, 253 (2013)
[26] M. Cacciari, M. Greco, P. Nason, JHEP **05**, 007 (1998), hep-ph/9803400
[27] M. Cacciari, S. Frixione, P. Nason, JHEP **03**, 006 (2001), hep-ph/0102134
[28] R. Sharma, I. Vitev, B.W. Zhang, Phys. Rev. **C80**, 054902 (2009), arXiv:0904.0032
[29] Z.B. Kang, I. Vitev, E. Wang, H. Xing, C. Zhang, Phys. Lett. **B740**, 23 (2015), arXiv:1409.2494
[30] A.M. Sickles, Phys. Lett. **B731**, 51 (2014), arXiv:1309.6924
[31] B. Abelev, etal, Journal of High Energy Physics **2012**, 1 (2012)
[32] J. Adam et al., (ALICE Collaboration), JHEP **07**, 051 (2015), arXiv:1504.07151
[33] S. Chatrchyan et al., (CMS Collaboration), JHEP **05**, 063 (2012), arXiv:1201.5069
[34] V. Khachatryan et al., (CMS Collaboration), Eur. Phys. J. **C71**, 1575 (2011), arXiv:1011.4193
[35] G. Aad et al., (ATLAS Collaboration), Nucl. Phys. **B850**, 387 (2011), arXiv:1104.3038
[36] D. Acosta et al., (CDF Collaboration), Phys. Rev. **D71**, 032001 (2005), hep-ex/0412071
[37] P. Antonioli, A. Kluge, W. Riegler (ALICE Collaboration), Tech. Rep. CERN-LHCC-2013-019. ALICE-TDR-015 (2013), https://cds.cern.ch/record/1603472
[38] B. Abelev et al., (ALICE Collaboration), Tech. Rep. CERN-LHCC-2013-024. ALICE-TDR-017 (2013), https://cds.cern.ch/record/1625842

[39] B. Abelev et al., (ALICE Collaboration), Tech. Rep. CERN-LHCC-2015-001. ALICE-TDR-018 (2015), https://cds.cern.ch/record/1981898